



# Condition monitoring of Mechanical Subsystems of Agricultural Vehicles Based on Fusion of Vibration Features

D. Moshou<sup>1</sup>, D. Kateris<sup>1</sup>, N. Sawalhi<sup>4</sup>, I. Gravalos<sup>2</sup>, S. Loutridis<sup>3</sup>, T. Gialamas<sup>2</sup>,  
P. Xyradakis<sup>2</sup>, Z. Tsiropoulos<sup>2</sup>

<sup>1</sup>Aristotle University, School of Agriculture, Agricultural Engineering Laboratory, Thessaloniki, Greece,

<sup>2</sup>Technological Educational Institute of Larissa, Department of Biosystems Engineering, Larissa, Greece

<sup>3</sup>Technological Educational Institute of Larissa, Department of Electrical Engineering, Larissa, Greece

<sup>4</sup>School of Mechanical and Manufacturing Engineering, University of New South Wales, Sydney, Australia



## Introduction

Bearings are located at the heart of rotating machinery and play a very important role in industrial applications and are mainly used to support and fix the axle in rotating machinery.

Their failure in practical operation can lead to the breakdown of the whole machine. Accordingly, to increase reliability and reduce loss of production condition monitoring of bearing gets more and more important in recent years.

The use of vibration signals is quite common in the field of condition monitoring and fault diagnosis of bearings (Xu et al., 2009). To inspect raw vibration signals, a wide variety of techniques have been introduced that may be categorized into two main groups: classic signal processing (McFadden and Smith, 1984) and intelligent systems (Paya et al., 1997).





## Material and methods



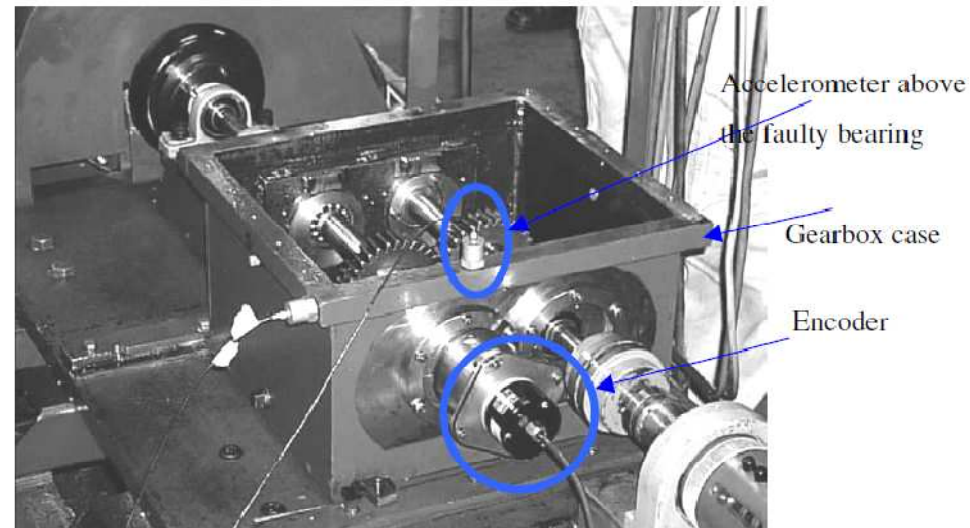
**Example of an extended fault in the inner race.**





## Material and methods

A gearbox test rig has been used in order to collect signals from different types of bearing faults. A photograph of the rig showing the position of the accelerometers and the encoder at the output shaft is shown in Figure (Sawalhi, 2007).

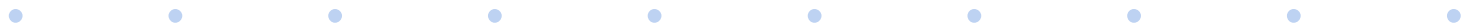




## Material and methods

Two types of faults (inner race and outer race crack) were tested under a 50 Nm load, while setting the output shaft speed to 10 Hz (600 rpm). Vibration signals were collected using two accelerometers positioned on the top of the gearbox casing above the defective bearing (vertical accelerometer) and sideways respectively (horizontal accelerometer).

The 1.35 seconds (65536 samples) signals were sampled at 48 kHz. A photo-reflective switch was placed near the output shaft to measure its speed by providing a once per rev tacho signal. The torque for each case was measured at the input shaft.





## Signal processing and feature determination

Feature extraction was performed using seven features. The first six features were introduced in (Lei et al., 2009): Kurtosis, Skewness, Crest, Clearance, Shape and Impulse Indicators.

- A newly proposed feature consisting of the line integral of the acceleration signal is introduced in this work.

All the used features provide statistical information about the nature of data, and were found to be reasonably good features for bearing fault detection.

The Kurtosis is the fourth moment about the mean normalized with variance and for a sliding window of  $N$  sampling points





## Features

$$Kurtosis = \frac{\sum_{i=1}^N (x_i - \mu_X)^4}{N\sigma_X^4} \quad (1)$$

$$Skewness = \frac{\sum_{i=1}^N (x_i - \mu_X)^3}{N\sigma_X^3} \quad (2)$$

$$Crest Indicator = \frac{\max |x_i|}{\sqrt{\frac{1}{N} \sum_{i=1}^N (x_i)^2}} \quad (3)$$

$$Clearance Indicator = \frac{\max |x_i|}{\left( \frac{1}{N} \sum_{i=1}^N \sqrt{|x_i|} \right)^2} \quad (4)$$

$$Shape Indicator = \frac{\sqrt{\frac{1}{N} \sum_{i=1}^N (x_i)^2}}{\frac{1}{N} \sum_{i=1}^N |x_i|} \quad (5)$$

$$impulse Indicator = \frac{\max |x_i|}{\sqrt{\frac{1}{N} \sum_{i=1}^N |x_i|}} \quad (6)$$

In equations (1)-(6) the symbols  $\mu_X$  and  $\sigma_X$  refer to mean value and standard deviation.



## Proposed feature “Line Integral”

$$LI = \int_a^b ds \approx \sum_{i=1}^N \|\vec{r}(t_i + T_s) - \vec{r}(t_i)\| = \sum_{i=1}^N \sqrt{(x(t_i + T_s) - x(t_i))^2 + T_s^2} \quad (7)$$
$$\approx \sum_{i=1}^N |x(t_i + T_s) - x(t_i)|$$

where

N is the number of sample points (equal to 500) in the window used to calculate Kurtosis and the other features and the newly proposed line integral feature,

$T_s$  is the sampling period.

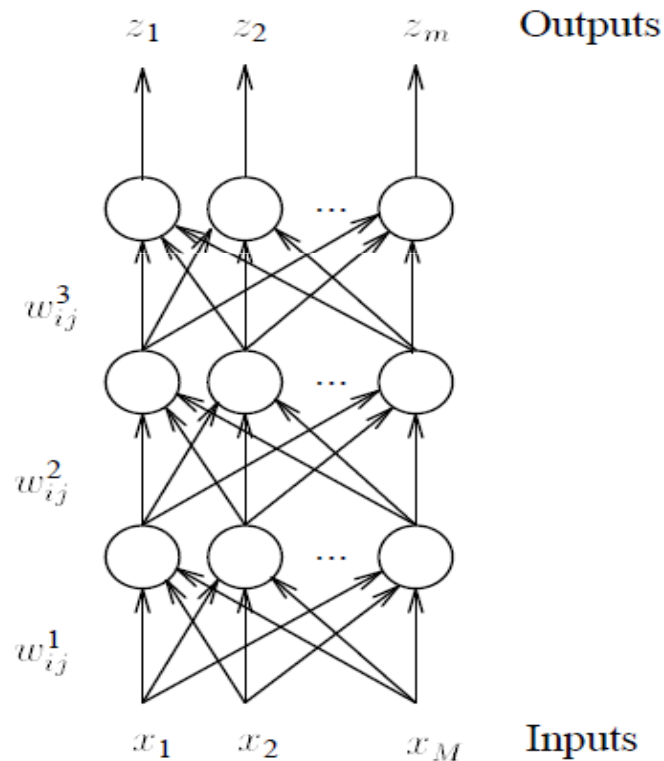
Given the high sampling rate of 48 kHz and the domination of the signal from high frequencies (especially due to the presence of faults), the final approximation contains only acceleration values. The feature vectors are then fed to the MLP for training.







## Neural network approach for monitoring fault topography



A general structure is shown in Figure.

The input to this network is the feature vector extracted from the object to be classified, and the output is typically a block code where one output is high indicating the class of the object and all other outputs are low.

The weights connecting the nodes are determined using some training rule with a set of feature vectors, the training set.



## Results and Discussion

For the experiments a multilayer perceptron with one hidden layer having 20 neurons was used.

A validation set was used to test the generalisation performance of the neural network.

To test the effectiveness of MLP, the 75% have been used for training while the 25% have been used in order to test the generalization of the MLP. The implementation used the Neural Net Matlab Toolbox (Mathworks).

The number of neurons in the input layer was equal to the number of used features. Different numbers of neurons in the hidden layer were used, varying between 5 and 25 at steps of 5.

Best results were obtained using a one hidden layer neural network with 20 neurons in the hidden layer, 14 inputs and three outputs (healthy - inner race - outer race) corresponding to fault position. The hidden layers and the output layer of the MLP had sigmoid neurons.



## Results and Discussion

Seven features of the same type from each accelerometer as shown in Table 1 according to order of presentation to the MLP. The same order has been used for the horizontal accelerometer in order to build the fusion vector.

Table 1. Ordering of the features for the vertical accelerometer as presented to the MLP.

1	2	3	4	5	6	7
Kurtosis	Line integral	Crest	Clearance	Shape	Impact	Skewness





## Results and Discussion

The fusion (by direct concatenation) of 14 vibration features from both the vertical and the horizontal accelerometer, due to their complementary nature, results in more accurate separation of classes regarding fault position as one can deduce from the results presented in following Tables which indicate the superiority of the fusion based classification result.

The order of presentation of the features is the following:

Results of classification of faults depending on their position by using a vertical accelerometer.  
The testing set used 25% of the data.

Vertical (% correct class estimate similar to fusion)		
100	0	0
0	96.8627	3.1373
0.3922	1.9608	97.6471



## Results and Discussion

Results of classification of faults depending on their position by using a horizontal accelerometer.  
The testing set used 25% of the data.

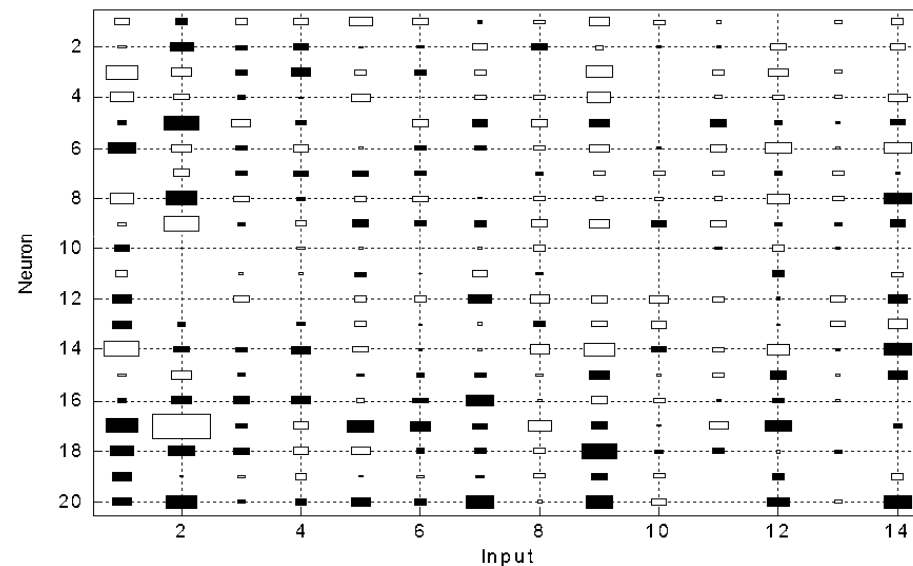
<b>Horizontal (% correct class estimate similar to fusion)</b>		
<b>84.7059</b>	<b>11.7647</b>	<b>0.7843</b>
<b>14.1176</b>	<b>87.8431</b>	<b>0.7843</b>
<b>1.1765</b>	<b>0.3922</b>	<b>98.4314</b>

Results of classification of faults depending on their position by using a vertical and a horizontal accelerometer and the fusion features from both. The testing set used 25% of the data.

<b>Fusion (% correct class estimate for healthy-inner race fault-outer race fault)</b>		
<b>100</b>	<b>0</b>	<b>0</b>
<b>0.392</b>	<b>99.608</b>	<b>0</b>
<b>0</b>	<b>0</b>	<b>100</b>



## Results and Discussion



The importance of different features can be determined qualitatively through a Hinton plot of the weight matrix as shown in Figure. The contribution of the **Kurtosis and Line integral** of the vertical accelerometer (**features 1 and 2**) and the **Line integral** of the horizontal (**feature 9**) is significant compared to the other features. Also, the **Shape Indicator and Skewness** of both accelerometers (**features 5, 7, and 12, 14**) contribute to the excitation of the hidden neurons and subsequently to the resulting classification. **Overall the Line integral shows the stronger contribution and from both accelerometers while the type of contribution is different per accelerometer indicating a complementary vibration component from each direction.**

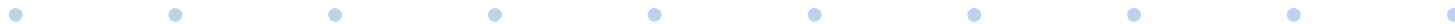


## Conclusions

It has been shown that the MLP can perform data fusion from accelerometer sensors through combining vibration features.

These features can be used to detect faults in roller bearings and discover the position of the faults, and can therefore prove to be a powerful tool for bearing health monitoring.

Different bearing faults can be detected with high accuracy by using the collective response of several features and the fusion of different sensors, which may not be obvious by just looking at the data using other diagnostic techniques.





## Conclusions

The use of kurtosis and a newly introduced feature, the line integral of the acceleration signal has given promising results in detecting the position of bearing faults.

The feature based fusion of the vertical and horizontal acceleration signals has increased the accuracy of fault detection to 99% for different fault types.

This result represented a substantial increase in discrimination performance of at least 10% for certain types of fault.

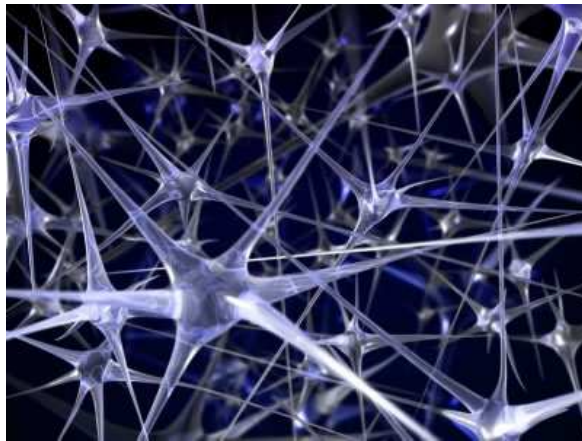
It is planned that this work be extended to include more real data, different features and spall sizes for bearings in gearboxes or other machines.

- 
- 
- 
- 
- 
- 
- 
- 
-





Thank you for your attention



**Condition monitoring of Mechanical Subsystems  
of Agricultural Vehicles Based on Fusion of Vibration Features**

